

IEEE International Conference on Mechatronics 2004

June 3 - 5, 2004

Istanbul / Turkey

ICM'04



IEEE Catalog Number: 04EX899C

ISBN: 0-7803-8600-0

ICM'04 CD PROCEEDINGS

Disclaimer

© 2004 IEEE. Personal use of this material is permitted. However, permission to reprint/republish this material for advertising or promotional purposes or for creating new collective works for resale or redistribution to servers or lists, or to reuse any copyrighted component of this work in other works must be obtained from the IEEE.

▪ **Main Menu**

Exit x

Pneumatic Force Control for Robotic Systems

H. Kazerooni,

Department of Mechanical Engineering
University of California, Berkeley, Berkeley, CA 94720
kazerooni@ME.BERKELEY.EDU

Abstract—This paper develops a control algorithm to convert a pneumatic actuator into a force generator. Since delivered power from a pneumatic actuator is product of the actuator force and the piston's displacement, through precise measurement of the piston's displacement and robust control of the actuator's power, one can effectively control the actuator force. This article first develops an exact model of a pneumatic system consisting of a double-acting cylinder and a servo-valve, with the goal of providing an insight into the design and control requirements for pneumatically-actuated systems. Using the model, derivation of a control algorithm that converts a pneumatic actuator into a force generator for robotics control applications is described.

I. INTRODUCTION

Well-known robotics control algorithms, such as computer torque method or sliding mode controllers, require the actuators to deliver well-regulated torque to the robot's joints. This concept originated from a practice, where most high performance robotic systems were designed to be powered by electric actuators. Although one can create a torque generator using current feedback of direct-drive electric motors, there are difficulties in transforming pneumatic actuators into force or torque generators. This is mostly due to the compressibility of air and nonlinearities in the servo-valves. Because of these difficulties, the early applications of pneumatic actuators were limited to simple and non-precise positioning applications, where actuators were controlled using on-off directional valves.

II. DERIVATION OF THE DYNAMICS OF A DOUBLE-ACTING ACTUATOR

The system consists of a double-acting linear pneumatic cylinder, fed by a 4-way servo servo-valve as shown in Figure 1. Assuming a control volume encompassing both chambers of the cylinder, and Chamber 1 is used as the intake chamber, the first law of thermodynamics is represented by equation (1):

$$\dot{Q} + \dot{m}_1 \left(h_{enter} + \frac{v_{enter}^2}{2} \right) = \dot{m}_2 \left(h_{exit} + \frac{v_{exit}^2}{2} \right) + \frac{\partial E}{\partial t} + \dot{W} \quad (1)$$

where:

\dot{Q} is the heat rate to the control volume

\dot{W} is the work rate (power) delivered by the control volume to the piston assembly

$\frac{\partial E}{\partial t}$ is the rate of change of the total energy of the control volume (both chambers).

\dot{m}_1 is the mass flow rate entering the control volume.

\dot{m}_2 is the mass flow rate exiting the control volume

h_{enter} is the enthalpy of gas entering Chamber 1 (right after the servo-valve or just before going to Chamber 1).

v_{enter} is the velocity of gas entering chamber 1 (right after the servo-valve or just before going to Chamber 1).

h_{exit} is the enthalpy of the gas exiting chamber 2 (right after Chamber 2 or just before going to servo-valve).

v_{exit} is the velocity of the gas exiting chamber 2 (right after Chamber 2 or just before going to servo-valve).

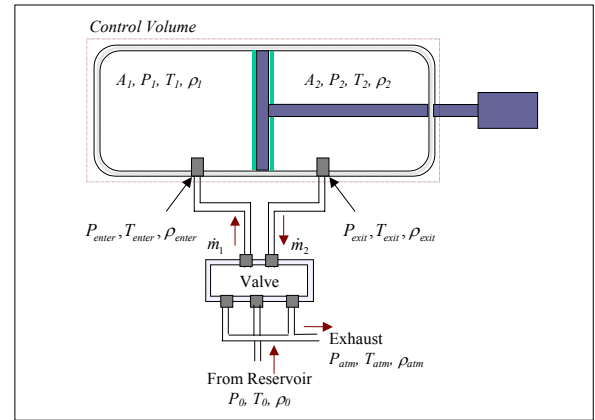


Figure 1. The Schematic of a Pneumatic Double Acting Actuator and a Servo-valve

Below we derive accurate equations for various elements of equation (1).

A. Derivation of $\frac{\partial E}{\partial t}$

The rate of change in kinetic and potential energies of the control volume are assumed small in comparison to the rate of change of the corresponding internal energy and is thus omitted. Therefore, the rate of change in the total energy of the control volume is:

$$\frac{\partial E}{\partial t} = \frac{\partial(U_1)}{\partial t} + \frac{\partial(U_2)}{\partial t} \quad (2)$$

where U_1 and U_2 are the internal energies of Chamber 1 and Chamber 2 respectively and are defined by Equations (3) and (4), assuming ideal gas is used for the system;

$$U_1 = C_V \rho_1 V_1 T_1 \quad (3)$$

$$U_2 = C_V \rho_2 V_2 T_2 \quad (4)$$

where V_1 , T_1 , ρ_1 , V_2 , T_2 and ρ_2 are volume, temperature and density associated with the gas in Chambers 1 and 2 respectively. Alternatively, equations (3) and (4) can be written as:

$$U_1 = \left(\frac{C_V}{R}\right) P_1 V_1 \quad (5)$$

$$U_2 = \left(\frac{C_V}{R}\right) P_2 V_2 \quad (6)$$

where P_1 and P_2 are the pressures in Chambers 1 and 2. C_V is the specific heat at constant volume and R is the gas constant. Substituting for U_1 and U_2 from equations (5) and (6) into equation (2) result in equation (7) for the rate of change in energy of the control volume.

$$\frac{\partial E}{\partial t} = \left(\frac{C_V}{R}\right) (\dot{P}_1 V_1 + P_1 \dot{V}_1) + \left(\frac{C_V}{R}\right) (\dot{P}_2 V_2 + P_2 \dot{V}_2) \quad (7)$$

B. Derivation of \dot{W}

The work rate done on the piston assembly by the gas in the pneumatic actuator is:

$$\dot{W} = P_1 \dot{V}_1 + P_2 \dot{V}_2 \quad (8)$$

where \dot{V}_1 and \dot{V}_2 are the rates of change of the volume of Chambers 1 and 2 respectively.

C. Derivation of Input and Output Enthalpies

The gas entering the actuator comes from a reservoir (usually an accumulator connected to an air compressor). Since the gas in the reservoir has zero velocity, its enthalpy is represented by the stagnation enthalpy h_o . Equation (9) describes the relationship between the stagnation enthalpy h_o and the enthalpy of the gas entering Chamber 1.

$$h_{enter} + \frac{v_{enter}^2}{2} = h_o = C_P T_o \quad (9)$$

where T_o is the temperature of the gas in the accumulator. C_P , the specific heat at constant pressure, is related to the aforementioned gas constants by $C_P = C_V + R$. Similarly, the velocity of the gas in Chamber 2 is very small in comparison to the velocity of the gas exiting through the servo-valve (v_{exit}). With this assumption, equation (10) relates the enthalpy of Chamber 2, h_2 , to the enthalpy of the gas exiting the servo-valve.

$$h_{exit} + \frac{v_{exit}^2}{2} = h_2 = C_P T_2 \quad (10)$$

where T_2 is the temperature of the gas in Chamber 2. Note the intake and exhaust enthalpies in equations (9) and (10) are based solely on their upstream gas temperatures.

D. Reevaluation of Equation 1

Substituting for $\partial E/\partial t$ from equation (7) and for the entering and existing energies from equations (9) and (10) into equation (1) result in equation (11):

$$\begin{aligned} \dot{Q} + \dot{m}_1 (C_P T_o) = \dot{m}_2 (C_P T_2) \\ + \left(\frac{C_V}{R}\right) (\dot{P}_1 V_1 + P_1 \dot{V}_1) + \left(\frac{C_V}{R}\right) (\dot{P}_2 V_2 + P_2 \dot{V}_2) + \dot{W} \end{aligned} \quad (11)$$

Further substitution for \dot{W} from equation (8) and simplification of terms result in equation (12):

$$\begin{aligned} \dot{Q} + \dot{m}_1 (C_P T_o) = \dot{m}_2 (C_P T_2) + \left(\frac{C_V}{R}\right) (\dot{P}_1 V_1 + \dot{P}_2 V_2) \\ + \left(1 + \frac{C_V}{R}\right) (P_1 \dot{V}_1 + P_2 \dot{V}_2) \end{aligned} \quad (12)$$

Assuming very little heat exchange between the actuator and its surrounding, equation (13) represents the first law of thermodynamics for the actuator:

$$\dot{m}_1 (RT_o) = \dot{m}_2 (RT_2) + \left(\frac{1}{k}\right) (\dot{P}_1 V_1 + \dot{P}_2 V_2) + (P_1 \dot{V}_1 + P_2 \dot{V}_2) \quad (13)$$

where $k = C_P / C_V$.

Let's assign the origin ($X = 0$) to be the far left end of the actuator in Figure 1, and L as the actuator's stroke length. The chamber volumes are:

$$\begin{cases} V_1 = A_1 X \\ V_2 = A_2 (L - X) \end{cases} \quad (14)$$

The derivatives of the chamber volumes are:

$$\begin{cases} \dot{V}_1 = A_1 \dot{X} \\ \dot{V}_2 = -A_2 \dot{X} \end{cases} \quad (15)$$

Substituting equations (14) and (15) in equation (13) results in equation (16):

$$\begin{aligned} \dot{m}_1 (RT_o) - \dot{m}_2 (RT_2) = \left(\frac{1}{k}\right) (\dot{P}_1 A_1 - \dot{P}_2 A_2) X \\ + \left(\frac{1}{k}\right) \dot{P}_2 A_2 L + (P_1 A_2 - P_2 A_2) \dot{X} \end{aligned} \quad (16)$$

Equation (16) states how X , mass position, varies as one modulates the mass flow rates, \dot{m}_1 and \dot{m}_2 , as a function of the servo-valve opening. In other words, \dot{m}_1 and \dot{m}_2 are considered two inputs to the system and one can control them directly to alter the position of the piston rod. Derivation of \dot{m}_1 and \dot{m}_2 requires the derivation of the dynamics of the pneumatic servo-valves, which will be addressed below.

III. DERIVATION OF THE DYNAMICS OF THE SERVO-VALVES

A converging nozzle fed from a large reservoir is considered a good model for the servo-valve. This converging passage discharges into Chamber 1 of the cylinder, where the pressure is P_1 (see Figure 2). It is assumed that the gas flow in the servo-valve is adiabatic everywhere, and the flow is isentropic everywhere except across the normal shock waves. In practice the servo-valves usually get warm and release heat to their surroundings. Therefore, the adiabatic assumption of the gas flow through a converging nozzle may not be an accurate representation of the gas' behavior in the servo-valve. In order to derive a set of equations that can be used for control purposes, we need to consider this discrepancy as model uncertainty and hope that the feedback control in the system minimizes the presence of this uncertainty in the system. The possible flow patterns in the servo-valve can now be investigated based on the values of the cylinder pressure, P_1 and the supply pressure P_o :

$$\text{Case 1: No-flow condition: } \frac{P_1}{P_o} = 1$$

In this case, the cylinder pressure (P_1) and the supply pressure (P_o) are equal. No flow takes place in the servo-valve from supply pressure to the cylinder. The load on the piston is so large that the piston does not move even when the servo-valve is fully open.

$$\text{Case 2: Sub-critical flow regime: } 0.53 < \frac{P_1}{P_o} < 1$$

If the servo-valve is opened slightly, then there will be a flow with a constantly decreasing pressure through the nozzle. Since the flow is subsonic at the exit plane, the throat pressure P_T must be the same as the cylinder pressure P_1 . It has been shown experimentally that the pressure in the pipe from the servo-valve down to the cylinder is equal to the cylinder pressure. Thus, the pressure is uniform and equal to P_1 from near the end of the servo-valve down to the cylinder chamber.

$$\text{Case 3: Critical flow regime } \frac{P_1}{P_o} = 0.53$$

As the difference between the supply pressure and the cylinder pressure increases, the stream velocity at the throat increases, until the point where the flow reaches its critical regime. At this point, the velocity of the gas in the throat is equal to the speed of sound calculated at the throat, and would never get larger even if the pressure difference increases.

$$\text{Case 4: Supercritical flow regime } \frac{P_1}{P_o} < 0.53$$

Further reducing the pressure in the cylinder will not affect the flow state at the throat due to choked flow in the servo-valve. In this regime, the pressure of the jet leaving the nozzle is greater than the cylinder pressure P_1 . The sudden reduction in pressure causes the jet to expand in an explosive fashion.

The pressure at throat P_T stays constant at $0.53P_o$. This situation is quite common and occurs when there is little load on the piston, and when P_1 is much smaller than P_o .

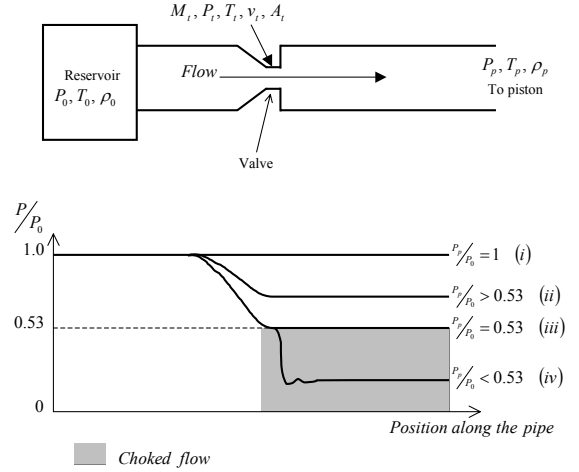


Figure 2. A converging nozzle fed from a large reservoir is considered a good model for the servo-valve. Other types (e.g. converging-diverging nozzles) were also investigated. However, the above converging nozzle was proven to be the most accurate model through experimental observation.

Our experiments also showed that, when the gas flow is under-choked, the pressure at the throat and the pressure in the cylinder are equal. When the gas flow is choked, the pressure at the throat stays constant at $0.53P_o$, whereas the cylinder pressure decreases more. The derivation of \dot{m}_1 and \dot{m}_2 as a function of the gas properties at the throat is straightforward. But the derivation of \dot{m}_1 and \dot{m}_2 , as a function of the cylinder pressure, need to be developed for both choked or under-choked gas flow in the servo-valve. Note that the pressure in each chamber can be measured, but the pressure at the throat of the servo-valve cannot be measured. The values for the pressure, density, and temperature of the gas flowing through the throat of the servo-valve can be calculated from equations (17), (18), and (19), regardless of the flow condition in the servo-valve.

$$\frac{P_T}{P_o} = \left(1 + \frac{k-1}{2} M_T^2 \right)^{\frac{k}{1-k}} \quad (17)$$

$$\frac{\rho_T}{\rho_o} = \left(1 + \frac{k-1}{2} M_T^2 \right)^{\frac{1}{1-k}} \quad (18)$$

$$\frac{T_T}{T_o} = \left(1 + \frac{k-1}{2} M_T^2 \right)^{-1} \quad (19)$$

The mass flow rate at the throat of the servo-valve is defined as:

$$\dot{m}_1 = \rho_T A_T v_T \quad (20)$$

where ρ_T and v_T are the density and velocity of the gas at the servo-valve throat. The velocity of the gas flow at the

throat can be calculated from the definition of the Mach number M_T as follows:

$$v_T = M_T \sqrt{k R T_T} \quad (21)$$

Substituting equations (17), (18), (19) and (21) into equation (20) gives the following expression for flow rate in terms of the servo-valve opening, the Mach number of the flow at the throat, and the reservoir properties:

$$\dot{m}_1 = M_T \left(1 + \frac{k-1}{2} M_T^2 \right)^{\frac{k+1}{2(1-k)}} \cdot \rho_o \cdot \sqrt{k R T_o} \cdot A_T \quad (22)$$

$$\text{or: } \dot{m}_1 = M_T \left(1 + \frac{k-1}{2} M_T^2 \right)^{\frac{k+1}{2(1-k)}} \cdot \sqrt{\frac{k}{R T_o}} \cdot P_o \cdot A_T \quad (23)$$

The value of \dot{m}_1 depends on the exact Mach number at the throat M_T , and the servo-valve opening A_T . Inverting equation (17) gives the expression for the Mach number as a function of the pressure at the throat P_T :

$$M_T = \sqrt{\frac{2}{k-1} \cdot \left(\left(\frac{P_T}{P_o} \right)^{\frac{1-k}{k}} - 1 \right)^{\frac{1}{2}}} \quad (24)$$

Substituting for M_T from equation (24) into equation (23) results in equation (25), which expresses the mass flow rate as a function of the gas properties in the reservoir, the pressure at the throat, and the throat opening:

$$\dot{m}_1 = \sqrt{\frac{2}{k-1} \left(\frac{P_T}{P_o} \right)^{\frac{k+1}{2k}} \cdot \left(\left(\frac{P_T}{P_o} \right)^{\frac{1-k}{k}} - 1 \right)^{\frac{1}{2}}} \cdot \sqrt{\frac{k}{R T_o}} \cdot P_o \cdot A_T \quad (25)$$

Expression (25) is valid for the gas entering the cylinder, regardless if the flow is choked or under-choked. In order to eliminate the only remaining unknown P_T , let's define γ_1 as

$$\gamma_1 = \sqrt{\frac{2}{k-1} \cdot \left(\frac{P_T}{P_o} \right)^{\frac{k+1}{2k}} \cdot \left(\left(\frac{P_T}{P_o} \right)^{\frac{1-k}{k}} - 1 \right)^{\frac{1}{2}}} \quad (26)$$

Therefore, equation (25) for mass flow rate can be written as:

$$\dot{m}_1 = \gamma_1 \cdot \sqrt{\frac{k}{R T_o}} \cdot P_o \cdot A_T \quad (27)$$

Now let us consider the following two cases:

Case 1: Under-choked gas flow

When the flow is under-choked, the pressure at the throat is equal to the cylinder pressure. Therefore γ_1 is given by equation (26):

$$\gamma_1 = \sqrt{\frac{2}{k-1} \cdot \left(\frac{P_1}{P_o} \right)^{\frac{k+1}{2k}} \cdot \left(\left(\frac{P_1}{P_o} \right)^{\frac{1-k}{k}} - 1 \right)^{\frac{1}{2}}} \quad (28)$$

Case 2: Choked gas flow

When the throat is choked, the pressure at the throat stays constant. In this case, P_1 stays constant and is equal to $0.53P_o$. Substituting for P_1 into equation (28) results in equation (29).

$$\gamma_1 = 0.58 \quad (29)$$

Therefore, the expression of the mass flow rate for gas entering the cylinder depends on whether the flow is choked or under-choked. Expression (30) summarizes the above results:

$$\dot{m}_1 = \gamma_1 \cdot \sqrt{\frac{k}{R T_o}} \cdot P_o \cdot A_T \quad (30)$$

if $P_1 > 0.53P_o$ (under-choked), then

$$\gamma_1 = \sqrt{\frac{2}{k-1} \cdot \left(\frac{P_1}{P_o} \right)^{\frac{k+1}{2k}} \cdot \left(\left(\frac{P_1}{P_o} \right)^{\frac{1-k}{k}} - 1 \right)^{\frac{1}{2}}} \quad (31)$$

if $P_1 \leq 0.53P_o$ (choked), then $\gamma_1 = 0.58$ (32)

As can be seen from equation (30), the mass flow rate is a function of the pressure reservoir and valve opening. Factor, γ_1 , can be illustrated as part of the 'gain' of the throat opening in the mass flow rate expression. At low cylinder pressure values, P_1 , this gain is constant ($\gamma_1 = 0.58$).

The outgoing mass flow rate can be derived similarly, but the second chamber is now taken as a "reservoir".

$$\dot{m}_2 = \gamma_2 \cdot \sqrt{\frac{k}{R T_2}} \cdot P_2 \cdot A_T \quad (33)$$

if $P_{atm} > 0.53P_2$ (under-choked), then

$$\gamma_2 = \sqrt{\frac{2}{k-1} \cdot \left(\frac{P_{atm}}{P_2} \right)^{\frac{k+1}{2k}} \cdot \left(\left(\frac{P_{atm}}{P_2} \right)^{\frac{1-k}{k}} - 1 \right)^{\frac{1}{2}}} \quad (34)$$

if $P_{atm} \leq 0.53P_2$ (choked), then $\gamma_2 = 0.58$ (35)

Equation (16), (30) and (33) constitute the equations for a cylinder and a servo-valve. A_T is considered an input to the system while P_1 , P_2 , \dot{m}_1 , \dot{m}_2 and X are unknown. The above equations can be used on two occasions: Control and Design.

IV. USE OF EQUATIONS FOR CONTROL

The goal of this section is to derive a control algorithm that converts a pneumatic actuator to a regulated force generator. By force generator we mean an actuator that uses feedback to impose a precise force as a function of an input command signal. This is important for robotic control systems since most robotic control algorithms assume the robot actuators are force/torque generating systems capable of imposing exact forces/torques. To stay consistent with the conventions made

previously, A_T , an algebraic area representing the area of servo-valve opening, is positive for gas entering the actuator. Most servo-valve manufacturers supply a small controller with their servo-valves so the users can accurately control the opening of the servo-valves by applying the correct voltage to the servo-valve controller. Here we assume such servo-valve controller is available and therefore the servo-valve opening, A_T , is proportional with a voltage command signal within a reasonably wide bandwidth. The objective is then to arrive at a practical control algorithm to convert a servo-valve and an actuator (similar to system of Figure 1) into a force-generating system, such that the force imposed by the actuator becomes proportional to the servo-valve opening, A_T , within a bounded bandwidth. To develop such system, we start from equation (16):

$$\begin{aligned} \dot{m}_1(RT_o) - \dot{m}_2(RT_2) = & \left(\frac{1}{k}\right) (\dot{P}_1 A_1 - \dot{P}_2 A_2) X \\ & + \left(\frac{1}{k}\right) \dot{P}_2 A_2 L + (P_1 A_2 - P_2 A_2) \dot{X} \end{aligned} \quad (16)$$

Using equations (30), (33), the servo-valve equation is presented by equation (36).

$$\dot{m}_1(RT_o) - \dot{m}_2(RT_2) = (\gamma_1 \sqrt{kRT_o} P_o - \gamma_2 \sqrt{kRT_2} P_2) A_T \quad (36)$$

where γ_1 and γ_2 can be calculated from equations (31), (32), (34) and (35) depending on the values of $\frac{P_1}{P_o}$ and $\frac{P_{atm}}{P_2}$.

Assume the force the piston imposes on the mass is presented by $F_p = P_1 A_1 - P_2 A_2$. Equating equations (16) and (36) results in the following expression for (F_p) , the piston force, as a function of the servo-valve opening, (A_T) :

$$(\gamma_1 \sqrt{kRT_o} P_o - \gamma_2 \sqrt{kRT_2} P_2) A_T = \left(\frac{1}{k}\right) \dot{F}_p X + F_p \dot{X} + \left(\frac{1}{k}\right) \dot{P}_2 A_2 L \quad (37)$$

Equation (37) relates the actuator force, (F_p) to (A_T) , the servo-valve opening. (A_T) is considered an input while (F_p) is the output to be controlled. Since this relationship is nonlinear, the implementation of a linear controller directly on the actuator force, without further control compensation, results in inadequate force tracking for the actuator. This lack of good force tracking behavior (e.g large error and low bandwidth) motivated us to investigate other possibilities for controlling the actuator force as described below.

The gas constant for air, (k) , is equal to 1.4 if the gas expansion process in the actuator is adiabatic. If gas expansion process is considered isentropic (constant temperature), then $k=1$. In reality, (k) is a number between 1 and 1.4 because the gas expansion in many applications is neither adiabatic nor isentropic. For example, if a pneumatic cylinder is well insulated and the system is designed to have a high bandwidth of operation (so gas has little time to release its energy to its surrounding), then one can comfortably assume the process is adiabatic and $k=1.4$. On other hand, if the

system has very little insulation or if the gas expansion is slow (so gas has ample time to exchange energy with its surrounding) then gas remains at a relatively constant temperature (Isentropic) where (k) can be assumed unity. Through our experiments, we noticed that our cylinder (similar to many other industrial pneumatic systems) became warm and exchanged heat with its surrounding since it had very little insulation. Therefore we judged (k) to be closer to unity than 1.4, and felt rather comfortable with the assumption of $k=1$. However, regardless of the assumption on the choice of (k) , we hope that the feedback in the system (described below) minimizes the effect of this modeling uncertainty at the output.

Assuming $k=1$, equation (37) can be written:

$$(\gamma_1 \sqrt{kRT_o} P_o - \gamma_2 \sqrt{kRT_2} P_2) A_T = \frac{d}{dt} (F_p X) + \dot{P}_2 A_2 L \quad (38)$$

Note how (X) and (F_p) are multiplied together in equation (38) to form an isolated variable. This prompts us to develop a controller to control and regulate $(F_p X)$ instead of (F_p) . Now we choose (A_T) to be equal to the following equation:

$$A_T = \frac{u + \dot{P}_2 A_2 L}{(\gamma_1 \sqrt{kRT_o} P_o - \gamma_2 \sqrt{kRT_2} P_2)} \quad (39)$$

where (u) is a control variable. Substituting for (A_T) from equation (39) into equation (38) results in equation (40) for the system.

$$u = \frac{d}{dt} (F_p X) \quad (40)$$

Assuming $(F_p X)$ as the variable to be controlled, the system presented by equation (40) seems like a first order linear system, where it can be stabilized with a PD or many other linear controllers. In general, we choose a linear transfer function for the controller, such that:

$$u(s) = K(s)(F_{Desired} X - F_p X) \quad (41)$$

to stabilize the system presented by equation (40), where $(F_{Desired})$ is the desired force. The term $(F_p X)$ is precisely equal to the work extracted from the piston and equation (41) prescribes a controller for its regulation. At first glance, the above controller may not seem satisfactory since the work, not the force, is being controlled (i.e. regulated) and therefore the accuracy of the force depends on the precision and accuracy of the piston's position (X) . In other words, no matter how accurately $(F_p X)$ is controlled (i.e. regulated by $K(s)$), (F_p) may be inaccurate due to the existence of noise and other uncertainties in measuring (X) . Although this is true in general, the piston's position, (X) is a very well-measured quantity and can be measured to a very high precision with little noise. Our experiments confirmed that controlling the piston work (i.e., $F_p X$) was practically the same as controlling

the force (F_p) if a high-precision encoder is used for measuring the piston position.

The experimental set-up of Figure 3 was used to verify the theories described here. The piston's location was calculated using precise measurement of the joint angle (4000 lines/revolution encoder) and geometrical knowledge of the system. An in-line force sensor was mounted right on the piston to measure the force on the piston rod. Two pressure sensors were mounted on both sides of the piston to measure the pressure in both chambers. The measurements of these pressure sensors were used not only in equation (39), but also to identify the existence of the choked flow in the servo-valve.

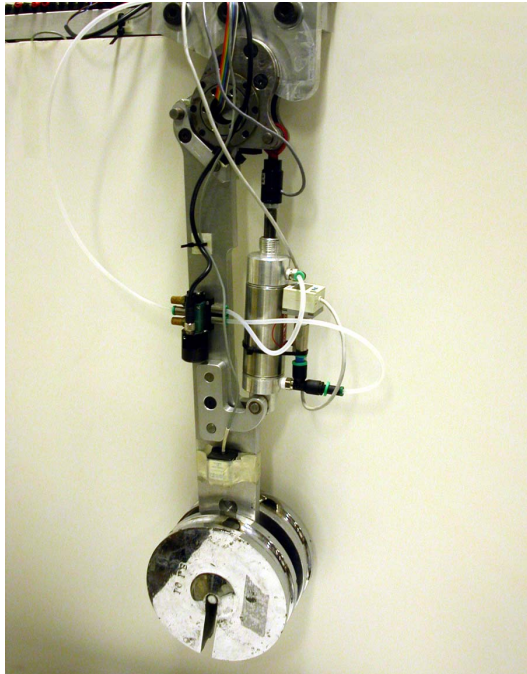


Figure 3. The Schematic of a Pneumatic Double-Acting Actuator and a Servo-valve

The experiments showed that the system was able to achieve torque tracking capability of up to about 10 Hz. Figure 4 shows the ratio of the actual measured torque over the desired torque at various frequencies, where the system response attenuates at frequencies above 10 Hz. This was rather encouraging for us, since our previous attempts for torque control without the use of the model described here never allowed good tracking at frequencies above 3 Hz. We believe this is due to accurate modeling of various phenomena in the servo-valve and the cylinder. We also learned that the most important point in creating a high-bandwidth force controller is not the choice of the controller $K(s)$ but the exact state of the air flow in the servo-valve (i.e. choked, critically choked or under choked). In other words, one must install precise pressure sensors on both sides of the cylinder to exactly identify if the flow is choked or under choked, and choose appropriate equations for the controller.

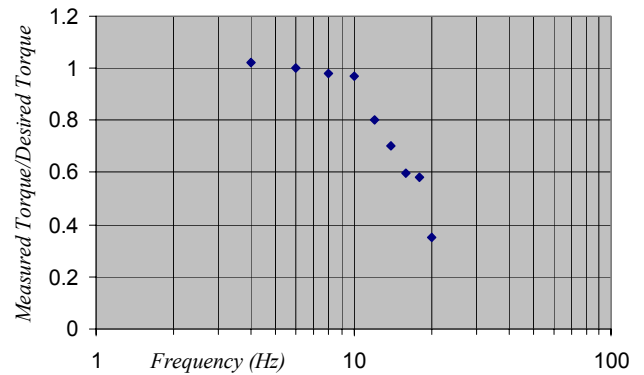


Figure 4. The system is able to track torque profiles up to 10 HZ.

CONCLUSION

One of the difficulties with pneumatic actuation is the compressibility of the gas, which causes the airflow through the servo-valve to be characterized as either a *choked* or *under-choked* flow. This paper models this phenomenon to arrive at a controller that turns a pneumatic cylinder and a servo-valve into a force generator for robotics applications. The control design method takes advantage of simplicity of the model when power is considered as an output. Since delivered power from a pneumatic actuator is product of the actuator force and the piston displacement, by precise measurement of the piston displacement and robust control of the actuator power, one can effectively control the actuator force. Through experiments we were able to arrive at 10Hz bandwidth force generator for a linear actuator.

REFERENCES

- [1] S. Liu and J.E. Burrows, "A analysis of a pneumatic Servo System and its Application to a Computer-Controlled Robot", ASME J. Dynam. Syst., Meas., Cont., Vol.110, pp.228-235, 1988.
- [2] J. E. Bobrow and F. Jabbari, "Adaptive Pneumatic Force Actuation and Position Control", ASME, J. of Dynamic Systems, Measurement and Control, June 1991, vol. 113.
- [3] Richer, E. and Hurmuzlu, Y., 2000, "A High Performance Pneumatic Force Actuator System: Part I-Nonlinear Mathematical Model" ASME J. of Dynamic Systems, Measurement, and Control, vol. 122, no. 3, pp. 416-425.
- [4] Ben-Dov, D., and Salcudean, S.E., 1995, A Force-Controlled Pneumatic Actuator, IEEE Transactions on Robotics and Automation, Vol.11, No. 6, pp. 906-911.
- [5] Wang, J., Pu, J., and Moore, P., "A practical control strategy for servo-pneumatic actuator systems," Control Engineering Practice, vol. 7, pp. 1483-1488, 1999.
- [6] Maeda, S., Kawakami, Y., and Nakano, K., "Position Control of Pneumatic Lifters," Transactions of Japan Hydraulic and Pneumatic Society, vol. 30, no. 4, pp. 89-95, 1999.